

PLASTIC YIELD AND REVERSE YIELD WAVES GENERATED BY IMPULSIVE ELECTROMAGNETIC RADIATION†

L. W. MORLAND‡

University of California, San Diego, La Jolla, California

Abstract—Absorption of radiation through a thin layer adjacent to an irradiated, stress free, surface causes rapid heating and the generation of stress waves. Temperature rises sufficient to cause plastic yielding in the initial stress jump and reverse yielding during the subsequent wave propagation are considered under the assumption of uni-axial strain. An elastic-plastic wave solution is constructed and compared with the purely elastic solution. In particular the reduced compressive and tensile stresses in the outgoing wave, and the pulse spread, are illustrated.

1. INTRODUCTION

THE generation of stress waves by rapid, non-uniform, heating of a solid (or fluid) due to the penetration and absorption of electromagnetic radiation through a surface layer is now of practical interest. See, for example, recent wave investigations by Gournay [1] who uses dyes in a fluid to vary the absorption depth and hence the resulting pulse length and stress amplitudes. In materials partially transparent to optical frequencies, significant stress levels can be attained by the use of Q -switched lasers from which the radiation duration is of order 10^{-8} sec. For absorption depths greater than 10^{-1} cm (say) the total energy is absorbed before any appreciable propagation from the absorption layer takes place, and the initial stress rise is effectively instantaneous. Furthermore, on the time scale of wave propagation over several absorption depths the subsequent thermal diffusion is negligible, and if thermomechanical coupling is neglected the temperature may be assumed steady; alternatively, if coupling is included, adiabatic response may be assumed. The impulsive heating limit followed by steady temperature considerably simplifies the wave analysis, and was adopted by Morland [2] to demonstrate the main wave features in a linear thermoelastic material, and subsequently by Hegemier and Morland [3] for a thermal-viscoelastic material. In each case uni-axial displacement and a stress-free surface were considered, and both compressive and tensile stresses occur in the outgoing wave.

Assuming the possibility of similar absorption in metals at other frequency levels and with sufficient energy deposit to produce an initial stress rise initiating yield, an elastic-plastic analysis was presented by Morland [4]. Estimates of the required surface temperature rise were made on the basis of quasistatic, room temperature, yield data; but in turn such wave generation may provide measures of the yield stress for high rates of strain and rapid temperature rise. The solution [4] was restricted to an intermediate range of initial stress rise for which yield occurs, but not reverse yield. Here the wave analysis is extended to include a reverse yield region which forms away from the surface

† The results presented in this paper were obtained in the course of research sponsored under Contract No. N00014-67-A-0109-0003, Task NR 064-496 by the Office of Naval Research, Washington, D.C.

‡ Consultant. Permanent position: School of Mathematics and Physics, University of East Anglia, England.

if the initial (surface) stress rise exceeds the minimum level for yield by a factor 2 (assuming equal tensile and compressive yield stress). In consequence both compressive and tensile parts of the outgoing pulse attenuate.

Referring to [4] for the detailed formulation, a summary of the governing equations is now presented. Uni-axial displacement normal to the surface, $u(x, t)$, is assumed, where x denotes particle distance from the surface in the undeformed configuration and t denotes time. The temperature T , initially zero, has an instantaneous rise $T(x)$ at $t = 0$ due to the impulsive heating and then remains steady during the propagation times considered. Initially the material is stress free and, while the strain remains zero at $t = 0$, there is an instantaneous elastic build-up of isotropic pressure given by

$$\sigma(x, 0+) = \sigma_L(x, 0+) = -3K\alpha T(x), \quad (1.1)$$

where σ , σ_L denote respectively the principal (Cauchy) longitudinal and lateral stress components, K is the bulk modulus, and α is the coefficient of linear thermal expansion. The result (1.1) is trivially modified if K and α are functions of T . Further, the stress rate is continuously zero at $t = 0$ [2], so that

$$\frac{\partial \sigma}{\partial t}(x, 0+) = 0. \quad (1.2)$$

Subsequent elastic changes at a fixed particle x , at steady temperature $T(x)$, satisfy the longitudinal differential relation

$$\frac{d\sigma}{d\varepsilon} = K + \frac{4}{3}G, \quad (1.3)$$

where G is the shear modulus and ε is the single non-zero longitudinal strain measuring extension per unit current length.

Both the von Mises and Tresca yield criteria reduce to

$$\sigma - \sigma_L = \pm y(T), \quad (1.4)$$

where the yield stress in simple tension, y , is allowed to depend on temperature. Typical work-hardening dependence is shown by Morland [5] to make little contribution in this stress geometry, and is neglected. It is unlikely that the significant quasistatic dependence on temperature observed after long exposure [6] is reproduced within the wave travel times of order 10^{-6} sec, and while a dependence is allowed in the formal solution the examples presented assume constant y . Adjoining the postulate of plastic incompressibility leads to the longitudinal plastic relation at steady temperature:

$$\frac{d\sigma}{d\varepsilon} = K, \quad (1.5)$$

together with the positive plastic work requirement

$$\sigma - \sigma_L = \pm y \rightarrow d\sigma \geq 0. \quad (1.6)$$

The positive sign condition is designated as yield, and the negative sign condition as reverse yield, for descriptive convenience. Figure 1 shows the longitudinal stress-strain path for a particle at steady temperature T , where A denotes the state following the initial instantaneous stress build-up, and the moduli K , G are assumed constant. The one-way direction of the yield path QB and reverse yield path CD is indicated by the arrows, and

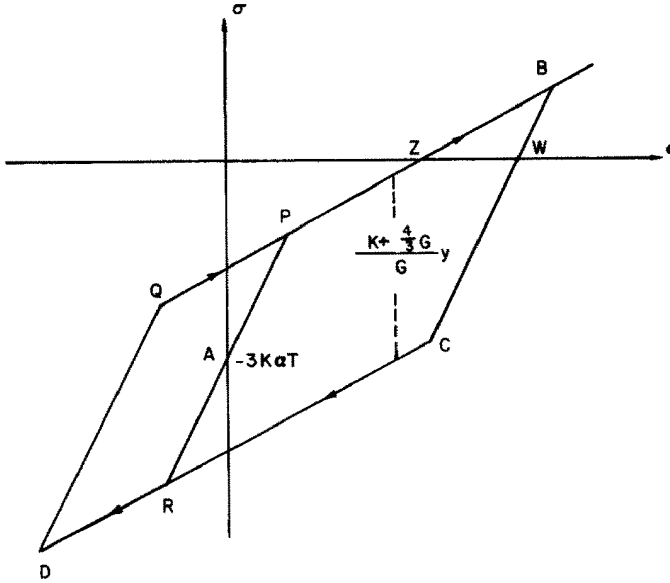


FIG. 1. Longitudinal stress-strain path at steady temperature T .

the elastic stress range between the two yield paths is

$$[\sigma] = (K + \frac{4}{3}G)y/G. \tag{1.7}$$

With the assumption of constant moduli K, G , and the small strain approximation

$$\epsilon = \frac{\partial u}{\partial x}, \tag{1.8}$$

the momentum equation reduces in continuous elastic and plastic regions to the wave equations

$$\frac{\partial^2 \sigma}{\partial x^2} = \frac{1}{c_i^2} \frac{\partial^2 \sigma}{\partial t^2} \quad (i = 1, 2). \tag{1.9}$$

c_0 and c_1 are respectively the elastic and plastic wave speeds given by

$$\rho c_0^2 = K + \frac{4}{3}G, \quad \rho c_1^2 = K (< \rho c_0^2), \tag{1.10}$$

where ρ is the initial uniform density. Finally, with a further postulate for instantaneous changes of state made by Morland and Cox [7], elastic and plastic stress discontinuities propagate with the speeds c_0 and c_1 respectively, and in particular a jump embracing both elastic and plastic changes splits into its separate parts.

2. WAVE PATTERN

First define dimensionless distance and time coordinates ξ, η by

$$x = l\xi, \quad t = l\eta/c_0, \tag{2.1}$$

where l is a measure of the absorption depth. Then the steady temperature distribution,

assumed to decrease monotonically to zero with depth, takes the form

$$T(x) = -T_M E(\xi); \quad E(0) = -1, \quad E(\xi) < 0, \quad E'(\xi) > 0; \\ E(\xi) \rightarrow 0 \quad \text{as} \quad \xi \rightarrow \infty. \quad (2.2)$$

Next define dimensionless stress $\theta(\xi, \eta)$, and effective yield stress $Y(\xi)$, by

$$\sigma = \sigma_M \theta, \quad (K + \frac{4}{3}G)y = 2G\sigma_M Y; \quad \sigma_M = 3K\alpha T_M. \quad (2.3)$$

The initial and boundary conditions then become

$$\theta(\xi, 0+) = E(\xi), \quad \frac{\partial \theta}{\partial \eta}(\xi, 0+) = 0; \quad \theta(0, \eta) = 0; \quad (2.4)$$

and the initial yield points P, R in Fig. 1 are given by

$$\theta(\xi, \eta) = E(\xi) \pm Y(\xi). \quad (2.5)$$

To achieve certain analytic conclusions we make the further postulates

$$E''(\xi) \leq 0, \quad E'''(\xi) \geq 0, \quad E'(\xi) \rightarrow 0 \quad \text{as} \quad \xi \rightarrow \infty, \quad (2.6)$$

which are satisfied by the example $E(\xi) = -e^{-\xi}$ used in the illustrations. In addition, from the common static observations [6] $y'(T) \leq 0, y''(T) \leq 0$, it follows that

$$Y'(\xi) \geq 0, \quad Y''(\xi) \leq 0; \quad Y'(\xi) \rightarrow 0 \quad \text{as} \quad \xi \rightarrow \infty. \quad (2.7)$$

In the new coordinates the elastic and plastic wave speeds are respectively

$$\frac{d\xi}{d\eta} = 1, \quad \frac{d\xi}{d\eta} = \frac{c_1}{c_0} = c < 1. \quad (2.8)$$

Across elastic and plastic stress discontinuities the jump conditions are respectively

$$[V] = -[\theta], \quad [V] = -[\theta]/c, \quad (2.9)$$

where the dimensionless particle velocity V is defined by

$$V = \frac{\rho c_0}{\sigma_M} \frac{\partial u}{\partial t}, \quad (2.10)$$

and in continuous regions

$$\frac{\partial V}{\partial \eta} = \frac{\partial \theta}{\partial \xi}. \quad (2.11)$$

Examination of the elastic solution [2] shows that, if $Y(0) < 1$, yield occurs at O , Fig. 2, behind the elastic characteristic OD , leading to a separation of the tensile jump into elastic and plastic parts propagating along OD, OA respectively. The solution constructed in [4], and illustrated by several examples, showed that yield did not occur at any particle ξ until reached by the plastic tensile jump propagating along OA , and subsequent to that jump the stress unloaded monotonically to zero. Thus, with the exception of the discontinuity path OA , the entire (ξ, η) domain was governed by the elastic equations. However, it was noted that if $Y(0) < 0.5$, reverse yield may, or may not, occur in the domain LOD , and certainly does if $Y(\infty) < 0.5$, and attention was

restricted to the intermediate range $0.5 \leq Y(0) < 1$. We will now consider a surface stress rise σ_M such that

$$Y(0) \leq Y(\infty) < 0.5. \tag{2.12}$$

With the postulates (2.6) it was shown [4] that reverse yield must first occur at some point R , Fig. 2, at the particle ξ_R , on the characteristic OD , ahead of the tensile jump, and subsequently a continuous elastic-plastic interface path RP is formed. Continuous interfaces of all six possible types are discussed in detail in [7]. Provided that the interface speed is not less than unity (the elastic wave speed), then classified as a super-fast elastic-plastic interface, the interface condition on RP is simply that the stress is at the initial reverse yield point for each particle ξ , represented by the point R in Fig. 1. Denoting the path RP by $\eta = \Psi(\xi)$ and using the known elastic solution in $LORP$, it follows that

$$E[\xi + \Psi(\xi)] + E[\xi - \Psi(\xi)] = 2E(\xi) - 2Y(\xi), \quad \xi \geq \xi_R; \quad \Psi(\xi_R) = \xi_R, \tag{2.13}$$

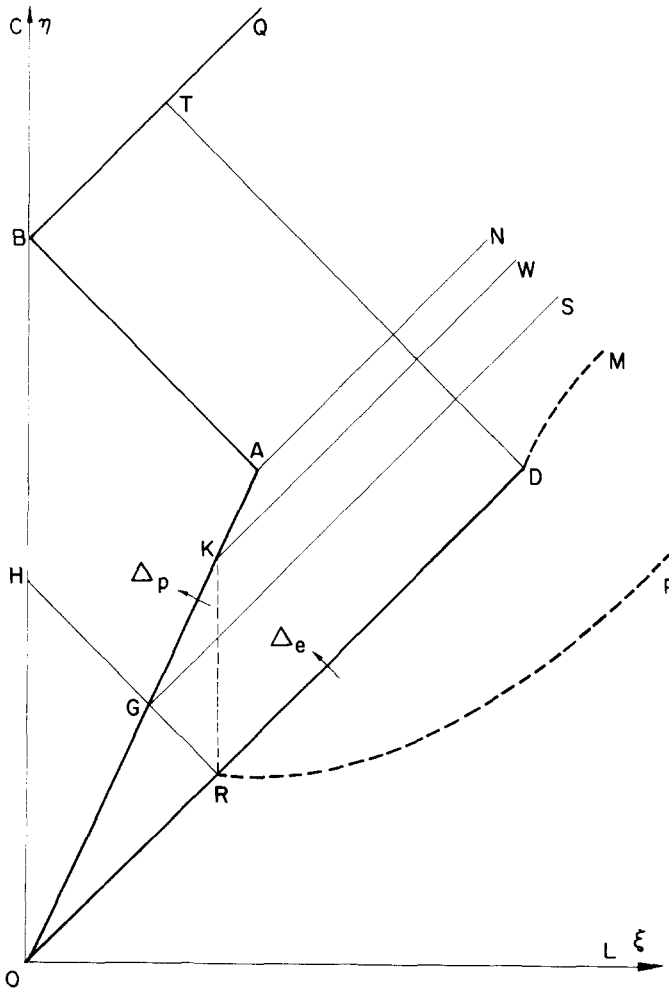


FIG. 2. Influence domains in the ξ, η plane; stress discontinuity paths shown —, continuous elastic-plastic interface paths shown - - - -.

which is an implicit equation for ξ_R and $\Psi(\xi)$. The postulates (2.6) guarantee [4] that $\Psi'(\xi) \geq 0$, and further, from the result

$$\Psi'(\xi) = 1 - \frac{2\{E'(\xi) - E'[\xi + \Psi(\xi)] - Y'(\xi)\}}{E'[\xi - \Psi(\xi)] - E'[\xi + \Psi(\xi)]}, \tag{2.14}$$

that $\Psi'(\xi) \leq 1$ if $Y'(\xi) = 0$. It may still follow if $y'(T) < 0$, but it is clear that if Y increases too rapidly with ξ a particle is reached beyond which the reverse yield condition cannot be attained by the stress distribution in *LOD*. We assume conditions are such that the required inequality,

$$\Psi'(\xi) \leq 1, \tag{2.15}$$

holds, trivial for constant Y .

In the later examples,

$$E(\xi) = -e^{-\xi}, \quad Y = \text{constant}, \tag{2.16}$$

(2.13) has the explicit solution

$$\Psi(\xi) = \cosh^{-1}\{1 + Ye^{\xi}\}, \quad \xi_R = -\log\{1 - (2Y)^{\frac{1}{2}}\}, \tag{2.17}$$

which has the properties

$$0 < \Psi'(\xi) < 1, \quad \Psi''(\xi) > 0, \quad \Psi'(\xi) \rightarrow 1 \quad \text{as} \quad \xi \rightarrow \infty. \tag{2.18}$$

These will be used to confirm results when general conclusions cannot be drawn.

There is a reverse yield domain *PRDM*, Fig. 2, in which each particle follows its path *RD*, Fig. 1, necessarily in the unloading (arrow) sense to meet the plastic work requirement (1.6). In this domain plastic waves formed on *RP* propagate in both directions, and continuity of stress and particle velocity across *RP* determines both wave functions; general conclusions regarding the unloading requirement will be obtained. Since a tensile jump propagates along the elastic characteristic *OR*, elastic reloading up a path *DQ*, Fig. 1, takes place discontinuously on *RD*, where *D* represents a point at which the discontinuity is supposed to be annulled. It is shown that for some range of Y satisfying (2.12) the discontinuity is not annulled in a finite distance. The wave pattern in Fig. 2 assumes that continuous elastic changes take place beyond *OD* until the plastic tensile jump path *OA* is reached, that is, remaining within the section *DQ*, Fig. 1, analogous to the solution [4] when reverse yield does not occur. The domain *ORH* is not influenced by the reverse yield waves.

At *OA*, ahead of the plastic discontinuity, the stress is at local yield, represented by the initial yield point *P*, Fig. 1, for $\xi \leq \xi_R$, but by the appropriate point *Q* for $\xi \geq \xi_R$, since reverse yield has previously occurred to the point *D*. Thus

$$\theta^-(\xi, \xi/c) = \begin{cases} E(\xi) + Y(\xi), & \xi \leq \xi_R \\ \theta^-(\xi, \xi) + 2Y(\xi), & \xi \geq \xi_R \end{cases} \tag{2.19}$$

where θ^- denotes stress ahead of a discontinuity. Relating the elastic stress and particle velocity jumps across *OD*, using (2.9), determines the stress jump $\Delta_e(\xi)$, and the backward elastic wave function in *DOA*, where the condition (2.19) determines the forward elastic wave generated at (reflected from) the slower plastic discontinuity. Finally, the jump relation across *OA* and boundary condition (2.4) on $\xi = 0$ determine the plastic stress

jump $\Delta_p(\xi)$ and the forward and backward elastic wave functions in the domain OAB , in which the stress is supposed to remain below yield. The solution behind the elastic jump is thus determined to the left of DT continued. Overall validity of this pattern rests on numerical solutions for individual examples.

It is shown that the plastic jump annulment point A occurs at a finite distance ξ_A , though not necessarily to the left of DT , as shown in Fig. 2, for all Y . When the elastic jump is annulled at a finite distance ξ_D , it is shown that the subsequent plastic-elastic interface cannot continue along the elastic characteristic OD extended, and further, that for some initial conditions $E(\xi)$, $Y(\xi)$, reverse yield continues to take place behind this characteristic, so that the interface must then follow a path DM as shown, slower than the elastic wave speed. For other initial conditions it may be faster than the elastic wave speed. The present solution is not extended beyond D . In the situation shown there is an expanding region of reverse yield, as RP and DM move further apart, but there the stress approaches a uniform level at the initial reverse yield stress and the plastic work approaches zero.

3. SOLUTION AND ILLUSTRATIONS

The formal solution is constructed by expressing the stress in the various influence domains of the ξ, η plane, Fig. 2, by appropriate pairs of wave functions. These are plastic in the reverse yield domain PRD , and elsewhere elastic except on the elastic and plastic discontinuity paths OD, OA respectively, across which the jump conditions (2.9) must be satisfied. Thus, after satisfying the initial and boundary conditions (2.4), the stress θ is given as follows:

$$LORP: \frac{1}{2}E(\xi + \eta) + \frac{1}{2}E(\xi - \eta). \tag{3.1}$$

$$PRD: \theta_R + f(\xi - c\eta) + g(\xi + c\eta), \quad \theta_R = E(\xi_R) - Y(\xi_R). \tag{3.2}$$

$$DOAN: k(\eta - \xi) + l(\xi + \eta). \tag{3.3}$$

$$OAB: j(\xi + \eta) - j(\eta - \xi). \tag{3.4}$$

θ_R denotes the stress at R ahead of the elastic discontinuity. The stress in other domains is given by extending the appropriate wave functions continuously across the domain boundaries, but only to the left of DT continued for $\eta > \xi$ if ξ_D is finite.

Applying the reverse yield condition on RP ,

$$\theta[\xi, \Psi(\xi)] = E(\xi) - Y(\xi), \quad \xi \geq \xi_R \tag{3.5}$$

and continuity of particle velocity, determines the two wave functions f, g :

$$f[\xi - c\Psi(\xi)] = \frac{1}{2}c\{1 + E[\xi - \Psi(\xi)]\} + \frac{1}{2}(1 - c)\{E(\xi) - Y(\xi) - \theta_R\}, \tag{3.6}$$

$$g[\xi + c\Psi(\xi)] = -\frac{1}{2}c\{1 + E[\xi - \Psi(\xi)]\} + \frac{1}{2}(1 + c)\{E(\xi) - Y(\xi) - \theta_R\}. \tag{3.7}$$

Differentiating (3.6), (3.7) and rearranging shows that

$$E'[\xi - \Psi(\xi)] - 2f'[\xi - c\Psi(\xi)] = \frac{(1 - c)\{E'[\xi - \Psi(\xi)] - E'(\xi) + Y'(\xi)\}}{1 - c\Psi'(\xi)} \geq 0 \tag{3.8}$$

on using the inequalities (2.18), (2.2), (2.6) and (2.7). Next differentiating (3.7),

$$f'[\xi - c\Psi(\xi)] - g'[\xi + c\Psi(\xi)] = \frac{c\{1 - \Psi'(\xi)\} \{E'[\xi - \Psi(\xi)] - E'(\xi) + Y'(\xi)\}}{\{1 - c\Psi'(\xi)\} \{1 + c\Psi'(\xi)\}} \geq 0. \tag{3.9}$$

Further differentiation of (3.6) gives

$$\begin{aligned} 2\{1 - c\Psi'(\xi)\}^2 f''[\xi - c\Psi(\xi)] &= -c\Psi''(\xi) \{E'[\xi - \Psi(\xi)] - 2f'[\xi - c\Psi(\xi)]\} \\ &\quad + c\{1 - \Psi'(\xi)\}^2 E''[\xi - \Psi(\xi)] \\ &\quad + (1 - c) \{E''(\xi) - Y''(\xi)\}. \end{aligned} \tag{3.10}$$

It follows from (2.13) that a necessary condition for $\Psi''(\xi) \geq 0$ is $E''(\xi) - Y''(\xi) \leq 0$, trivially satisfied if $Y''(\xi) = 0$ and otherwise imposing restrictions on $y'(T)$, $y''(T)$, so that in view of (3.8)

$$\Psi''(\xi) \geq 0 \rightarrow f''(\xi) \leq 0. \tag{3.11}$$

Recall that $\Psi''(\xi) \geq 0$ for the examples (2.16). For ξ, η in the domain *PRD*,

$$\begin{aligned} \frac{1}{c} \frac{\partial \theta}{\partial \eta} &= -f'(\xi - c\eta) + g'(\xi + c\eta) \\ &\leq -f'(\xi - c\eta) + f'(\Phi), \end{aligned} \tag{3.12}$$

for some $\Phi \geq \xi - c\eta$, using (3.9), and hence $\partial\theta/\partial\eta \leq 0$, as required to satisfy the unloading condition, when the implication (3.11) holds. Always

$$\frac{1}{c} \frac{\partial \theta}{\partial \eta} [\xi, \Psi(\xi)] = -f'[\xi - c\Psi(\xi)] + g'[\xi + c\Psi(\xi)] \leq 0. \tag{3.13}$$

Relating the stress and particle velocity jumps across *OD* gives

$$\Delta_e(\xi) = Y(0), \quad l(2\xi) = \frac{1}{2}E(2\xi), \quad \xi \leq \xi_R \tag{3.14}$$

$$\Delta_e(\xi) = Y(0) - \{(1 + c)f[(1 - c)\xi] - (1 - c)g[(1 + c)\xi]\}/2c, \quad \xi \geq \xi_R \tag{3.15}$$

$$l(2\xi) = \frac{1}{2}E(2\xi_R) + \{(1 + c)g[(1 + c)\xi] - (1 - c)f[(1 - c)\xi]\}/2c,$$

where $\Delta_e(\xi)$ and $l(2\xi)$ are continuous at $\xi = \xi_R$. The two domains for $l(\xi + \eta)$ are separated by the characteristic *RG*. Now for $\xi \geq \xi_R$,

$$\Delta'_e(\xi) = -(1 - c^2) \{f'[(1 - c)\xi] - g'[(1 + c)\xi]\}/2c, \leq 0 \tag{3.16}$$

for a valid plastic solution (3.12), and

$$\Delta_e(\xi_R) = Y(0) > 0, \quad \Delta_e(\xi) \rightarrow Y(0) + Y(\infty) - \frac{1}{2} \text{ as } \xi \rightarrow \infty. \tag{3.17}$$

Thus the condition for a finite ξ_D at which $\Delta_e(\xi_D) = 0$ is

$$\xi_D < \infty \Leftrightarrow Y(0) + Y(\infty) < 0.5, \tag{3.18}$$

and $\xi_D \rightarrow \infty$ if $Y(0) + Y(\infty) \geq 0.5$. In the case $Y = \text{const.}$ the critical value is $Y = 0.25$. Since the reverse yield solution is valid ahead of the elastic characteristic *OD* continued if (3.11) holds, independent of the position ξ_D , the continuation of the plastic-elastic interface path beyond a finite ξ_D must then be behind this characteristic, as represented by *DM*. Continuous interface conditions and solutions are discussed in detail in [7]; the present solution is not extended beyond *D*. However, it follows from (3.6), (3.7), using the postulate

(2.6), that within *PRDM*

$$\partial\theta/\partial\eta \rightarrow 0 \quad \text{as} \quad \xi \rightarrow \infty \tag{3.19}$$

so that at each ξ the stress approaches the initial local reverse yield point for all η and no plastic work is done.

Using the yield condition (2.19) on *OA*, ahead of the plastic discontinuity, gives

$$k[(1-c)\xi/c] = \theta^-(\xi, \xi/c) - l[(1+c)\xi/c]. \tag{3.20}$$

Dependence on the prior reverse yield enters through *l* beyond *GS*, and through θ^- beyond *KW* since the local yield point depends on the previous reverse yield stress for $\xi > \xi_R$. Now relating stress and particle velocity jumps across the plastic discontinuity path *OA* determines a difference equation for *j*:

$$j(z) - \delta j(\delta z) = G(z), \quad z \geq 0 \tag{3.21}$$

$$z = (1+c)\xi/c, \quad \delta = (1-c)/(1+c), \tag{3.22}$$

$$G(z) = \delta\theta^-(\xi, \xi/c) + (1-\delta)l(z) + \frac{1}{2}(1+\delta) - \delta Y(0).$$

For a typical value $c = 0.8$, $\delta \ll 1$ and the solution of (3.21) is simply a few terms of the iterated series

$$j(z) = \sum_{r=0}^{\infty} \delta^r G(\delta^r z). \tag{3.23}$$

Also the plastic stress jump is given by

$$\Delta_p(\xi) = \frac{G(z) - (1-\delta)j(z)}{\delta} - \theta^-(\xi, \xi/c). \tag{3.24}$$

As $\xi \rightarrow \infty$, $\theta^-(\xi, \xi/c) \rightarrow Y(\infty)$ and $(1-\delta)j(z) - G(z) \rightarrow 0$, so

$$\Delta_p(0) = 1 - Y(0) > 0, \quad \Delta_p(\xi) \rightarrow -Y(\infty) < 0 \quad \text{as} \quad \xi \rightarrow \infty, \tag{3.25}$$

and there exists a finite ξ_A at which Δ_p first becomes zero. For $\xi < \xi_A$, $\Delta_p(\xi) > 0$ and the plastic discontinuity meets the validity requirement (1.6). Validity beyond *OA* requires that the stress remains below the last plastic stress $\theta^+(\xi, \xi/c)$ behind the discontinuity *OA* for $\xi \leq \xi_A$, and for $\xi > \xi_A$ below the yield stress $\theta^-(\xi, \xi) + 2Y(\xi)$. Confirmation is obtained in the numerical examples where, in fact, monotonic unloading takes place. The general properties of *j(z)* deduced in [4] when no reverse yield occurs still apply in the domain *OGH*, in particular $j''(z) \leq 0$ which implies monotonic unloading.

Solutions are now presented for the examples (2.16) with various values of *Y* satisfying (2.12) and $c = 0.8$. The following table lists the respective ξ_R , where reverse yield first occurs, ξ_D where the elastic discontinuity is annulled, and ξ_A where the plastic discontinuity is annulled if this occurs, as represented in Fig. 2, in the solution domain bounded by *DT*. Also the location ξ_F and duration of reverse yield, $\xi_F - \Psi(\xi_F)$, when the slope $\Psi'(\xi)$ becomes effectively unity; both clearly increases with decrease of *Y*. This increase in reverse yield

<i>Y</i>	ξ_R	ξ_D	ξ_A	ξ_F	$\xi_F - \Psi(\xi_F)$
0.1	0.59	1.90		3.00	1.61
0.15	0.79	2.95		2.88	1.20
0.2	1.00	4.30		2.49	0.92
0.25	1.23	∞	5.45	2.32	0.69
0.3	1.49	∞	4.35	2.27	0.51

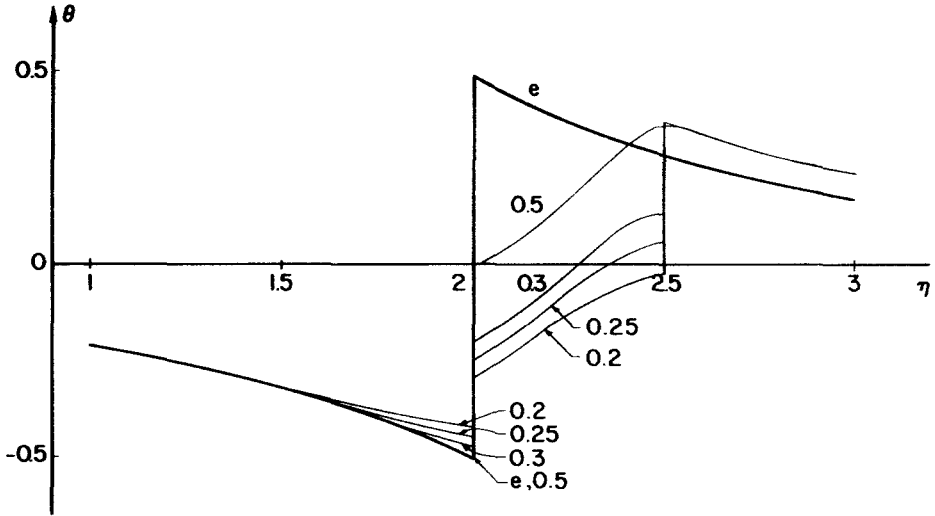


FIG. 3. Stress variation with time η at $\xi = 2$; elastic case (e) and plastic cases $Y = 0.5, 0.3, 0.25, 0.2$.

duration is accompanied by a faster attenuation of the elastic discontinuity and ξ_D decreases. The reverse trend is indicated for the annulment distance ξ_A of the plastic (tensile) discontinuity, to which may be added the results [4] $\xi_A = 1.98, Y = 0.5$; $\xi_A = 0.96, Y = 0.75$.

A comparison of the stress pulse at $\xi = 2$ for various values of Y , including the case $Y = 0.5$ [4], and the elastic solution [2], is shown in Fig. 3. Here the elastic pulse has effectively attained its final tensile and compressive amplitudes ± 0.5 (at the discontinuity), and the plastic tensile discontinuity for $Y = 0.5$ is annulled. Attenuation of the compressive stress ahead of the elastic discontinuity with decrease of Y below 0.5, due to reverse yield, is indicated, together with the different shape of loading beyond the elastic

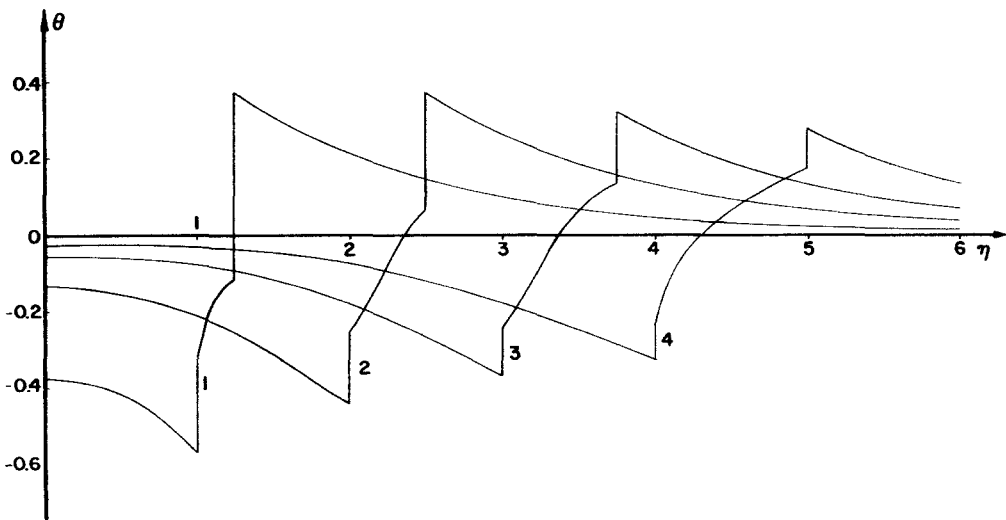


FIG. 4. Stress variation with time η at $\xi = 1, 2, 3, 4$; $Y = 0.25$.

discontinuity, still including the final plastic discontinuity for the values of Y below 0.5. The final (monotonic) unloading beyond $\eta = \xi/c$ is nearly identical for all the cases shown.

Figure 4 shows the stress pulse at locations $\xi = 1, 2, 3, 4$ for $Y = 0.25$. The tensile stress behind the plastic discontinuity in fact increases from zero at $\xi = 0$ to a maximum 0.38 at $\xi = 1.4$ and then decreases to the value 0.22 at $\xi_A = 5.45$. The compressive stress ahead of the elastic discontinuity decreases monotonically from -1 at $\xi = 0$ to a steady value -0.25 by $\xi = 10$. That is, both tensile and compressive amplitudes are eventually much lower than the levels ± 0.5 of the elastic solution, and there is the loading-pulse spread between $\eta = \xi$ and ξ/c in contrast to the totally discontinuous loading of the elastic solution. The maximum tensile stress is little affected by the reverse yield region, and for all the values of Y considered occurs between $\xi = 1.3$ and 1.5 and has magnitude approximately 0.38. Thus the significant effect is the attenuation in the ultimate outgoing wave beyond (say) ten absorption depths where the backward signals are negligible.

REFERENCES

- [1] L. S. GOURNAY, Conversion of electromagnetic to acoustic energy by surface heating. *J. acoust. Soc. Am.* **40**, 1322 (1966).
- [2] L. W. MORLAND, Generation of thermoelastic stress waves by impulsive electromagnetic radiation. *AIAA Jnl* **6**, 1063 (1968).
- [3] G. A. HEGEMIER and L. W. MORLAND, Stress waves in a temperature dependent viscoelastic half-space subjected to impulsive electromagnetic radiation. *AIAA Jnl* in press.
- [4] L. W. MORLAND, Elastic-plastic wave generation by impulsive electromagnetic radiation. *Int. J. Solids Struct.* **5**, 319 (1969).
- [5] L. W. MORLAND, The propagation of plane irrotational waves through an elastoplastic medium. *Phil. Trans. R. Soc.* **A251**, 341 (1959).
- [6] Military Handbook-5, *Metallic Materials and Elements for Flight Vehicle Structures*. Department of Defense, Washington, D.C. (1962).
- [7] L. W. MORLAND and A. D. COX, Existence and uniqueness of solutions to uniaxial elastic-plastic wave interactions. *Phil. Trans. R. Soc.* in press.

(Received 18 November 1968)

Абстракт—Абсорпция и радиация сквозь тонкий слой, примыкающий к облученной и свободной от напряжений поверхности, вызывает быстрый нагрев и образование волн напряжения. Исследуется повышение температуры, достаточное для образования пластического течения, в начале скачка напряжения и образования обратного течения, во время последующего распространения волны, предполагая одноосную деформацию. Дается решение упруго-пластической волны и сравнивается с чисто упругим решением. В качестве особого случая, иллюстрируются редуцированные напряжения сжатия и растяжения в исхочшей волне, а также распространение импульса.